

Available online at www.sciencedirect.com

SCIENCE @ DIRECT®

Thin Solid Films xx (2005) xxx – xxx

www.elsevier.com/locate/tsf

Characterisation of Pristine and Recoated electron beam evaporation plasma-assisted physical vapour deposition Cr–N coatings on AISI M2 steel and WC–Co substrates

J.C. Avelar-Batista ^{a,*}, E. Spain ^a, J. Housden ^a, G.G. Fuentes ^b, R. Rebolé ^b,
R. Rodriguez ^b, F. Montalá ^c, L.J. Carreras ^c, T.J. Tate ^d

^aTecvac Ltd, Buckingway Business Park, Swavesey, Cambridge, CB4 5UG, United Kingdom

^bCentre of Advanced Surface Engineering-AIN, San Cosme y San Damian s/n, E-31191 Pamplona, Spain

^cTratamientos Termicos Carreras, Avenida Can Rosés, Nave 8, Polígono Industrial Can Rosés, E-08191, Rubí, Barcelona, Spain

^dIC Consultants Ltd, Exhibition Road, London, SW7 2QA, United Kingdom (UK)

Received 3 December 2004; received in revised form 7 June 2005; accepted 10 June 2005

Abstract

This paper is focussed on the characterisation of electron beam evaporation plasma-assisted physical vapour deposition Cr–N coatings deposited on AISI M2 steel and hardmetal (K10) substrates in two different conditions: *Pristine* (i.e., coated) and *Recoated* (i.e., stripped and recoated). Analytical methods, including X-ray diffraction (XRD), scanning electron microscopy, scratch adhesion and pin-on-disc tests were used to evaluate several coating properties. XRD analyses indicated that both *Pristine* and *Recoated* coatings consisted of a mixture of hexagonal Cr₂N and cubic CrN, regardless of substrate type. For the M2 steel substrate, only small differences were found in terms of coating phases, microstructure, adhesion, friction and wear coefficients between *Pristine* and *Recoated*. *Recoated* on WC–Co (K10) exhibited a less dense microstructure and significant inferior adhesion compared to *Pristine* on WC–Co (K10). The wear coefficient of *Recoated* on WC–Co was 100 times higher than those exhibited by all other specimens. The results obtained confirm that the stripping process did not adversely affect the Cr–N properties when this coating was deposited onto M2 steel substrates, but it is clear from the unsatisfactory tribological performance of *Recoated* on WC–Co that the stripping process is unsuitable for hardmetal substrates.

© 2005 Elsevier B.V. All rights reserved.

Keywords: Wet stripping; Physical vapour deposition (PVD); Scanning electron microscopy; X-ray diffraction

1. Introduction

Plasma-Assisted Physical Vapour Deposition (PAPVD) processes have been commercially used to deposit chromium nitride (Cr–N) coatings on steel substrates. Among these processes, electron beam evaporation PAPVD (EB PAPVD) has been successfully used to produce Cr–N coatings, mainly due to its high deposition rates and excellent surface finish obtained in polished components.

Industrial applications of Cr–N coatings include cutting and forming tools, as well as injection-moulding dies for plastics [1–4]. Cr–N has favourable tribological properties (i.e., low friction coefficient and high wear resistance) [5–11], allied to good oxidation and corrosion resistance [10–17], and is a possible replacement for hard chromium. Nevertheless, the industrial demand for Cr–N on tungsten carbide tools is still small.

Cr–N coatings usually have fine-grained and low stress structure, so that thicker (up to 10–25 μm) can be deposited, compared to conventional PAPVD coatings of a few microns [2]. As Cr–N usually has lower hardness and higher toughness than TiN, they are often deposited on soft substrates such as stainless steel, copper and aluminium

* Corresponding author. Tel.: +44 1954 233700; fax: +44 1954 233733.

E-mail addresses: junia.avelar-batista@tecvac.com,
juniacri@yahoo.co.uk (J.C. Avelar-Batista).

alloys, which cannot provide enough support for more brittle and harder coatings [2,18].

Chromium nitride has two different crystalline phases: CrN (face centred cubic structure) and β -Cr₂N (hexagonal structure). Cr–N coatings can be prepared with a wide range of phase structures, having only a single phase (CrN or Cr₂N) or a mixed phase structure containing Cr and Cr₂N or Cr₂N and CrN, mainly depending on the nitrogen partial pressure [12,19–23]. Coatings having a single Cr₂N phase [5,12,19–25] have been found to be hardest, whereas coatings possessing Cr₂N and CrN phases with additional nitrogen [22] have highest internal stresses.

Cr–N coatings often provide good oxidation resistance up to 973–1073K [12,15–17,26], which is accomplished by the formation of a protective top Cr₂O₃ layer [17]. The CrN phase appears to provide a superior oxidation resistance than Cr or Cr₂N phases [12]. Cr–N coatings can also enhance the corrosion resistance of steel substrates [5,10,13,14]. Their corrosion resistance can be further enhanced by using interlayers such as metallic chromium [14], electroless nickel [27] and electroless nickel–phosphorous [28].

Paradoxically, the industrial use of Cr–N coatings on expensive or added value components is often limited by the good oxidation and corrosion resistance, making it difficult to strip without causing any damage to the substrate. As a new wet stripping process that causes little or negligible damage to steel substrates has been developed [29], it is relevant to compare some coating properties (crystalline phases, microstructure, adhesion and wear) for *Pristine* (i.e., coated) and *Recoated* (i.e., stripped and *Recoated*). In this paper, EB PAPVD Cr–N coatings deposited on AISI M2 steel and hardmetal (K10) substrates were characterised before, and after, stripping and recoating. Coating properties were evaluated using X-ray diffraction (XRD), scanning electron microscopy (SEM), scratch adhesion and pin-on-disc tests.

2. Experimental details

2.1. Materials and treatments

Cr–N was deposited on hardened and polished AISI M2 steel discs (60 HRC, 29.5 × 0.5 mm) and polished tungsten carbide (K10, nominal composition (wt. %): 92.7 WC; 1.0 TaC; 0.3 Cr₂C₃; 6.0 Co) discs (29.5 × 4.8 mm) by EB PAPVD using a Tecvac IP70L coater. All specimens were subjected to a 5 min sputter cleaning step before initiating coating deposition (*Pristine* specimens). Some Cr–N coatings on both M2 steel and tungsten carbide substrates were chemically stripped as described elsewhere [29]. The stripping solution consisted of KOH and a strong oxidising agent. After stripping, substrates were recoated in the same way as the *Pristine* specimens and, therefore, subjected to another 5 min sputter cleaning cycle (*Recoated* specimens).

The coating temperature was kept at 673–723 K for all coating cycles.

2.2. Coating characterisation

A Fischerscope X-ray XDL system was used to assess the coating thickness in all specimens. This system is an energy dispersive, high-performance X-ray fluorescence spectrometer and can detect elements from aluminium to uranium, even at very low concentrations (0.1–0.2 wt.%). Coating thickness or alloy composition is determined from the energy and intensity of the respective X-ray emission. The X-ray energy was set to 50 kV in all thickness measurements.

The scratch test method was used to assess coating adhesion. A CSEM Revetest scratch tester was used to perform the tests. The radius of the diamond indenter in the scratch test was 0.2 mm and the measurements were carried out at an increasing load rate of 10 N mm⁻¹. Three critical loads (L_{C1} , L_{C2} and L_{C3}) were determined from a set of three scratches on each specimen. L_{C1} was taken as the load at which cohesive failures occurred; L_{C2} the load corresponding to first occurrence of adhesive failure (i.e., the load at which the substrate was first exposed); and L_{C3} was the load at which the coating was completely removed from the scratch channel. The specimen surface and diamond tip were cleaned with isopropanol before each scratch. Although acoustic emission and frictional force were recorded during the tests, the critical loads were determined by optical microscopy.

Coating phase composition was investigated by means of XRD using Cu-K_α radiation ($\lambda=0.154056$ nm). The diffractograms were recorded with a 2θ step of 0.02°/s from 20° to 90°. Scanning electron microscopy (Cambridge Stereoscan 250 Mk2 scanning electron microscope) was used to investigate the surface and fracture cross-section morphology of the coatings at an accelerating voltage of 20 kV.

Pin-on-disc wear tests were performed using a Falex Isc-320pc tribometer, at ambient conditions. A 3 mm diameter WC–Co ball was used for the tests, which were set at a linear speed of 10 cm s⁻¹ and a load of 5 N. The wear coefficients were determined after a sliding distance of 1257 m (20,000 cycles). A Wyco RST 500 optical profilometer, using vertical scanning and phase shift interferometry to a vertical resolution better than 10 nm, was used to obtain 2D topographical images of the wear tracks. The images were obtained over a scanned area of 0.9 × 1.2 mm.

3. Results and discussion

3.1. Coating thickness

Coating thickness obtained from X-ray fluorescence measurements for both *Pristine* and *Recoated* on M2 steel

and WC–Co substrates, are shown in Table 1. All coatings on WC–Co have similar (within 10%) thicknesses, whereas on M2 steel, *Pristine* is 1.0 μm (66%) thicker than *Recoated*.

3.2. X-ray diffraction analyses

XRD patterns of *Pristine* and *Recoated* on M2 steel are illustrated in Fig. 1a, whereas those of *Pristine* and *Recoated* on WC–Co (K10) are shown in Fig. 1b. Both *Pristine* and *Recoated* crystallised into hexagonal Cr_2N and cubic CrN phases, regardless of substrate type. Diffraction peaks corresponding to the M2 steel or WC–Co substrate were also present. For *Recoated* on either M2 steel or WC–Co, the higher intensity of substrate peaks in comparison to those of the coating suggests that these films are thinner than the *Pristine* (see Table 1).

By comparing the line intensities to those of a random sample, it can be concluded that the cubic CrN phase in *Pristine* (either M2 steel or WC–Co substrates) has a major (200) preferred orientation ($I \text{CrN (111)}/I \text{CrN (200)}$) is 0.03 for M2 steel and 0.02 for WC–Co), whilst the hexagonal Cr_2N has a major (111) preferred orientation ($I \text{Cr}_2\text{N (002)}/I \text{Cr}_2\text{N (111)}$) is 0.04 for M2 steel and 0.02 for WC–Co). Other crystalline orientations become more significant in *Recoated* on both substrates, indicating that these coatings have a more random texture ($I \text{CrN (111)}/I \text{CrN (200)}$) is 0.23 for M2 steel and 0.39 for WC–Co and $I \text{Cr}_2\text{N (002)}/I \text{Cr}_2\text{N (111)}$) is 0.31 for M2 steel and 0.44 for WC–Co).

The randomisation of texture for both cubic and hexagonal chromium nitride phases might be related to the higher surface roughness that resulted from stripping in *Recoated* samples [29]. For a certain adatom energy, a high substrate roughness will influence coating growth by effectively reducing their mobility and the appearance of other crystalline orientations will be promoted.

3.3. SEM examination

SEM images of surface morphology and fracture cross-section of *Pristine* and *Recoated* are shown in Fig. 2a–h. The surface morphology indicates an increase in surface roughness for *Recoated* on M2 steel and WC–Co substrates (Fig. 2c and g respectively), as previously detected by surface roughness measurements [29]. Nevertheless, larger

Table 1
Coating thickness of *Pristine* and *Recoated* EB PAPVD Cr–N coatings deposited on M2 steel and WC–Co (K10) substrates

Specimen	Thickness ^a (μm)
<i>Pristine</i> on M2 steel	2.5 \pm 0.1
<i>Recoated</i> on M2 steel	1.5 \pm 0.1
<i>Pristine</i> on WC–Co (K10)	2.0 \pm 0.1
<i>Recoated</i> on WC–Co (K10)	1.8 \pm 0.1

^a Average thickness obtained from 5 measurements.

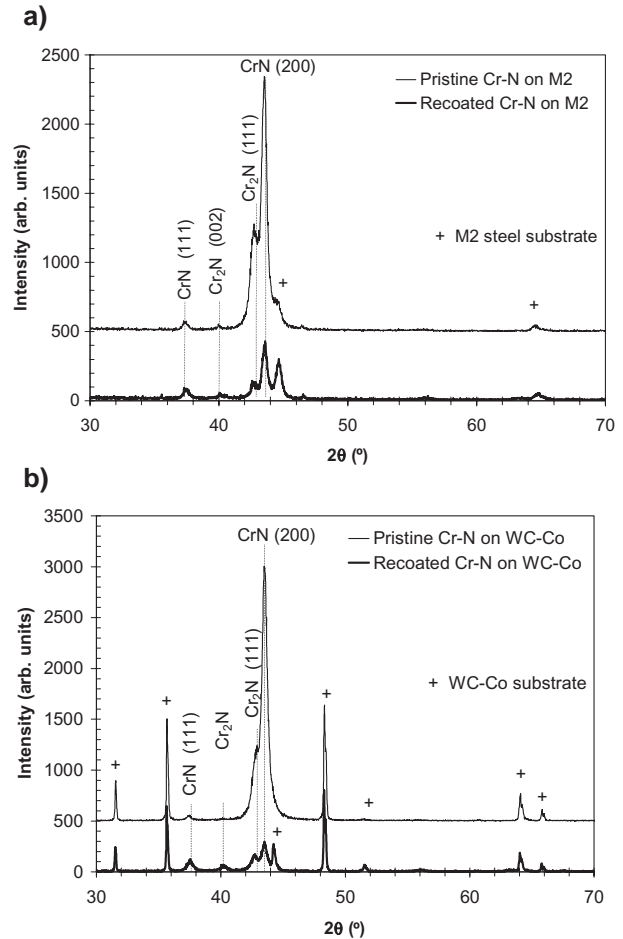


Fig. 1. XRD patterns of Cr–N coatings on (a) M2 steel and (b) WC–Co substrates in both *Pristine* and *Recoated* conditions. For clarity the diffractogram for *Pristine* coatings was shifted to higher intensities by 500 a.u.

defects/pores can be identified on the *Recoated* on WC–Co (Fig. 2g).

Fracture cross-sections of *Pristine* and *Recoated* on M2 steel (Fig. 2b and d respectively) reveal that both coatings have similar dense structures. Although their structure is columnar in nature, the high density results in unclear column boundaries, resembling the coating structure described as ‘Zone 2’ in Ref. [30].

The *Pristine* on WC–Co (Fig. 2f) also exhibits a dense film structure, similar to those found in *Pristine* and *Recoated* on M2 steel. However, the structure of *Recoated* on WC–Co is very distinctive, being less dense and having a granular appearance (Fig. 2h). Such a microstructure probably developed from coating growth on the damaged substrate, which had a high surface roughness (one order of magnitude higher than the other samples [29]).

3.4. Scratch tests

The critical loads for *Pristine* and *Recoated* are illustrated in Table 2. For *Pristine* on both substrates, cohesive failures (i.e., failures occurring within the coating)

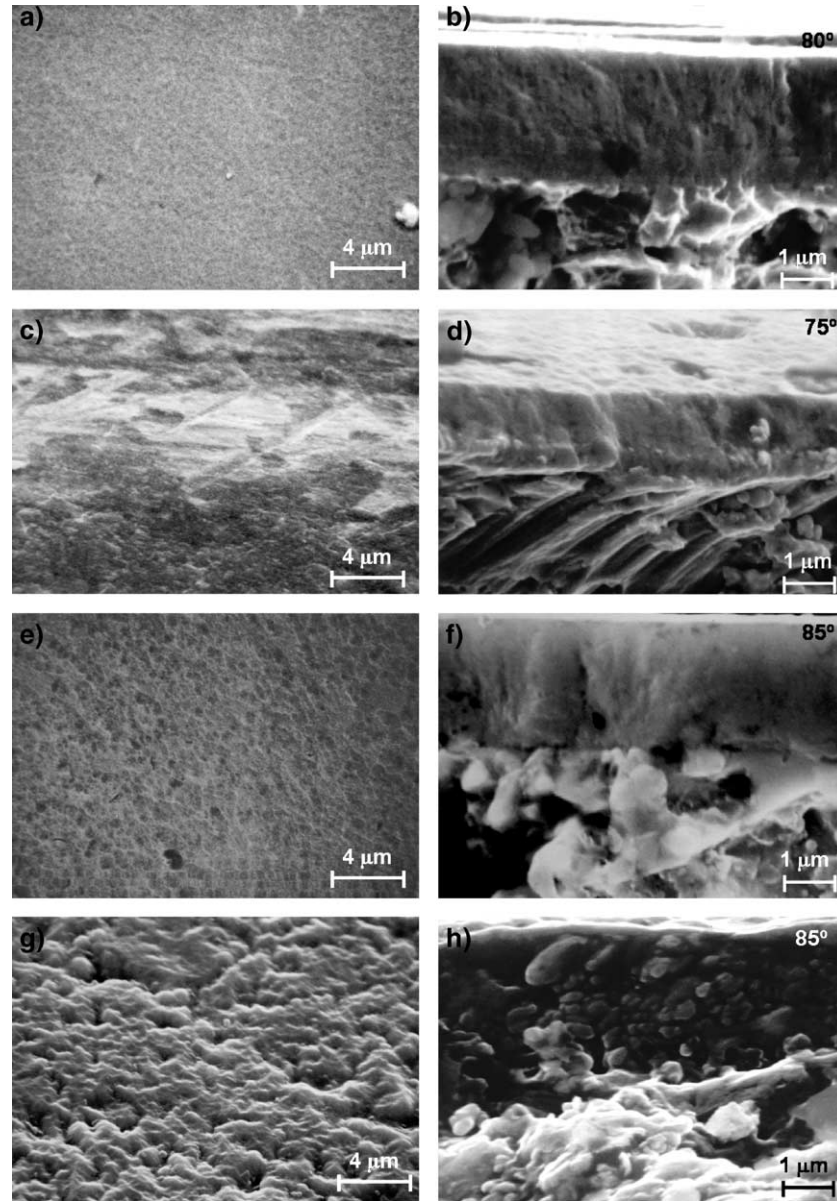


Fig. 2. Surface (a,c,e,g) and fracture cross-section (b,d,f,h) SEM images of Cr–N coatings on (a,b) *Pristine* M2 steel; (c,d) *Recoated* M2 steel; (e,f) *Pristine* WC–Co (K10) and (g,h) *Recoated* WC–Co (K10).

occurred in two different modes: cracking and chipping. Small cracks at the edge of the scratch channel start to develop at very low loads in these coatings. As the load increased, a pattern of semicircular cracks (tensile cracks) could be observed at the scratches [31]. The tensile cracking

mode is characteristic of well-adherent coatings [31]. The cracks form as a result of tensile stresses behind, balancing the compressive frictional stresses in front of, the trailing edge of the stylus [31]. Except for *Recoated* on WC–Co, chipping of the coating was a cohesive failure that could also be detected at higher loads.

For the M2 steel substrate, the difference in the critical loads of *Pristine* and *Recoated* is small. *Pristine* and *Recoated* displayed similar L_{C2} values, whilst higher L_{C1} chipping and L_{C3} values were recorded for *Recoated*, having a thickness of 1.5 μm . As an increase of critical loads with thickness is observed [32], the previous results suggest that the stripping process was not detrimental to the coating adhesion, as *Recoated* exhibited higher critical loads than *Pristine*.

Table 2
Critical loads obtained from scratch adhesion tests

Specimen	Critical loads (N)			
	L_{C1} cracking	L_{C1} chipping	L_{C2}	L_{C3}
<i>Pristine</i> M2 steel	12 \pm 1	31 \pm 3	60 \pm 3	92 \pm 5
<i>Recoated</i> on M2 steel	–	37 \pm 2	55 \pm 3	109 \pm 1
<i>Pristine</i> on WC–Co (K10)	22 \pm 2	33 \pm 4	109 \pm 14	115 \pm 15
<i>Recoated</i> on WC–Co (K10)	–	–	7 \pm 2	14 \pm 1

Table 3

Friction (μ) and wear coefficients (k) obtained for uncoated substrates, *Pristine* and *Recoated* coatings after pin-on-disc tests. Tests were performed using a 3 mm diameter WC–Co ball and 5 N applied load

Specimen	μ	k ($\text{m}^3 \text{N}^{-1} \text{m}^{-1}$)
Uncoated AISI M2 steel	0.6	7.0×10^{-16}
<i>Pristine</i> on M2 steel	0.5	2.4×10^{-16}
<i>Recoated</i> on M2 steel	0.3	3.2×10^{-16}
Uncoated WC–Co (K10)	0.4	$<1.0 \times 10^{-16}$
<i>Pristine</i> on WC–Co (K10)	0.3	$<1.0 \times 10^{-16}$
<i>Recoated</i> on WC–Co (K10)	0.3	2.9×10^{-14}

For the WC–Co substrate, very low critical loads were recorded for *Recoated* in comparison with *Pristine*. *Recoated* displayed only adhesive failures, indicating that the stripping process caused significant damage to the hardmetal substrate, as reported elsewhere [29].

It is interesting to note that *Pristine* on WC–Co showed higher critical loads than *Pristine* on M2 steel. This is probably due to the higher hardness of the hardmetal substrate in comparison to that of the M2 steel, which improves the load support for the Cr–N coating [33,34].

3.5. Pin-on-disc tests

Results from pin-on-disc tests are shown in Table 3. The friction coefficients exhibited the same order of magnitude as those reported for Cr–N films in the literature [35]. Regardless of substrate type, the decrease in the friction coefficient from *Pristine* to *Recoated* was very small.

All samples show high wear resistance ($1/k$), except *Recoated* on WC–Co (Table 3). The wear coefficient of the latter was ~ 100 times higher than those recorded for the other specimens, including both uncoated substrates. These results were corroborated by 2-D surface profilometry of the wear tracks (Fig. 3a–f). It is interesting to note that *Pristine* on WC–Co exhibited a higher wear resistance than *Pristine* on M2 steel. As the hardness and surface roughness of *Pristine* on both substrates were similar [29], the superior performance of the *Pristine* on WC–Co must be related to an improved load support from this substrate to the Cr–N coating, as evidenced by scratch test results.

The small increase in surface roughness for *Recoated* on M2 [29] was not detrimental to the tribological performance, as similar wear coefficients were obtained for *Pristine*

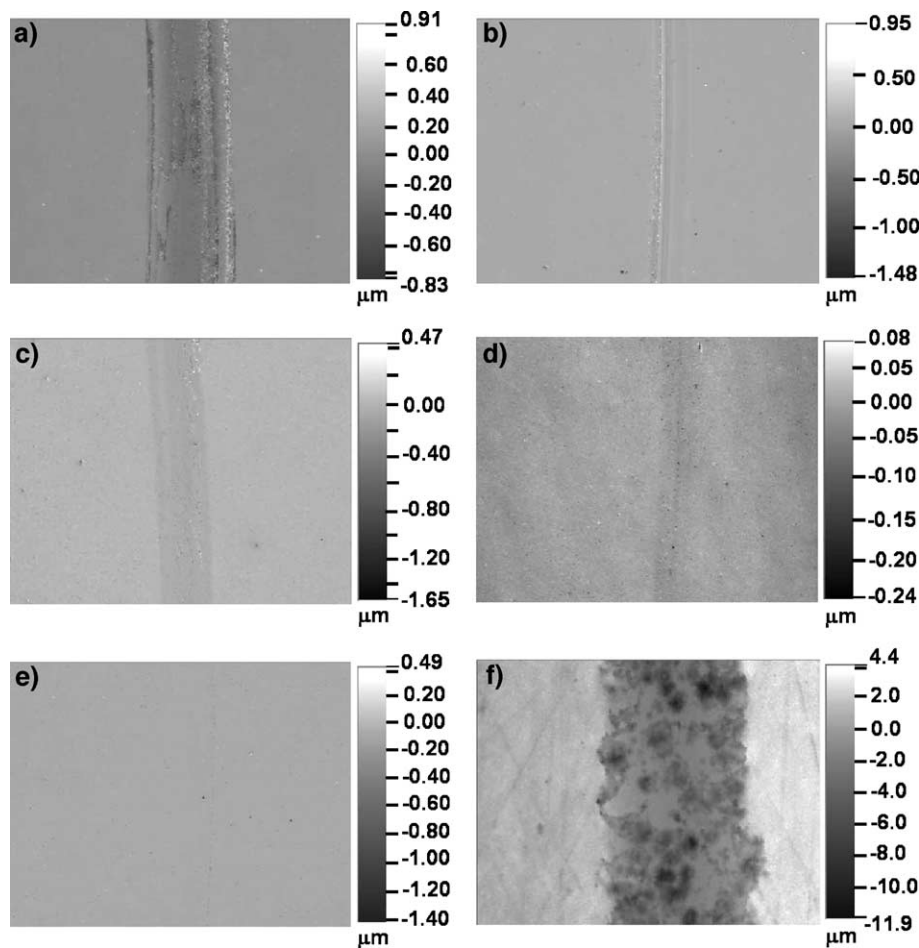


Fig. 3. 2-D topographical images of the wear tracks produced after pin-on-disc tests on: a) Uncoated M2 steel; (b) *Pristine* on M2 steel; (c) *Recoated* on M2 steel; (d) Uncoated WC–Co (K10); (e) *Pristine* on WC–Co and (f) *Recoated* on WC–Co. Tests were carried out using a 3 mm diameter WC–Co ball and 5 N applied load over a sliding distance of 1257 m.

and *Recoated* on M2 steel. Therefore, pin-on-disc results indicate that the tribological response of Cr–N coatings on M2 steel substrates was not adversely affected by the stripping process.

The unsatisfactory tribological response of *Recoated* on WC–Co probably results from its high surface roughness [29], low hardness [29] and poor adhesion (Table 2), showing that the stripping process caused significant damage to the WC–Co substrate.

3.6. Summary

Previous results obtained from glow discharge optical spectroscopy, surface roughness and ultra-microhardness measurements showed that the stripping process caused significant damage to the WC–Co substrate but not to the M2 steel substrate [29]. SEM results also indicated that the stripping process was detrimental to the WC–Co substrate, as evidenced by the less dense coating structure that resulted from recoating (*Recoated* sample). The similar performances achieved by *Pristine* and *Recoated* Cr–N on M2 steel in scratch adhesion and pin-on-disc wear tests further validate the stripping process for this substrate. Conversely, the unsatisfactory performance of *Recoated* Cr–N on WC–Co indicates that this stripping process cannot be used on carbide substrates.

4. Conclusions

Pristine and *Recoated* (i.e., stripped and then recoated) Cr–N coatings on M2 steel and WC–Co (K10) substrates were characterised using XRD, SEM, scratch adhesion and pin-on-disc wear tests. XRD analyses revealed that all *Pristine* and *Recoated* Cr–N coatings, regardless of substrate type, consisted of a mixture of hexagonal Cr₂N and cubic CrN phases. However, a more random texture resulted in the *Recoated* specimens. SEM examination of fracture cross-sections indicated that *Pristine* and *Recoated* Cr–N on M2 steel and *Pristine* on WC–Co had similar dense columnar structures. However, the coating structure in *Recoated* on WC–Co was less dense and had a granular morphology. Scratch test results revealed that the adhesion of *Recoated* on WC–Co was poor, as very low critical loads were recorded. The high critical loads obtained for the other coating/substrate systems indicated a satisfactory film/substrate adhesion. Although only small variations in the friction coefficient were detected from pin-on-disc wear tests among all Cr–N coatings and uncoated substrates (M2 steel and WC–Co), the wear rate of *Recoated* on WC–Co was ~100 times higher than all other coatings and uncoated substrates. The poor performance achieved by *Recoated* on WC–Co substrates in scratch adhesion tests and pin-on-disc tests invalidates the use of this stripping process on WC–Co substrates. Nevertheless, the similar tribological performances achieved by *Pristine* and *Recoated* on M2 steel

reinforces the suitability of the stripping process for steel substrates.

Acknowledgements

The authors are greatly indebted to: (i) the UK EUREKA Unit from the Department of Trade and Industry, for supporting the project CREST Σ! 2949 under the EUREKA program funding; (ii) Ministry of Industry and Technology of Spain through the PROFIT programme; (iii) the Government of Navarra for co-funding and (iv) P. Hunneyball of Tecvac Ltd. for the SEM photomicrographs.

References

- [1] P.A. Dearnley, *Wear* 225–229 (1999) 1109.
- [2] B. Navinsek, P. Pajan, I. Milosev, *Surf. Coat. Technol.* 97 (1997) 182.
- [3] M. Heinze, G. Mennig, G. Paller, *Surf. Coat. Technol.* 74–75 (1995) 658.
- [4] B. Navinsek, P. Pajan, *Surf. Coat. Technol.* 74–75 (1995) 919.
- [5] G. Bertrand, H. Mahdjoub, C. Meunier, *Surf. Coat. Technol.* 126 (2000) 199.
- [6] Y.L. Su, S.H. Yao, C.S. Wei, C.T. Wu, W.H. Kao, *Mater. Lett.* 35 (1998) 255.
- [7] Y.L. Su, S.H. Yao, Z.L. Leu, C.S. Wei, C.T. Wu, *Wear* 213 (1997) 165.
- [8] Y.L. Su, S.H. Yao, C.T. Wu, *Wear* 199 (1996) 132.
- [9] J.A. Sue, T.P. Chang, *Surf. Coat. Technol.* 76–77 (1995) 61.
- [10] L. Cunha, M. Andritschky, K. Pischow, Z. Wang, A. Zarychta, A.S. Miranda, A.M. Cunha, *Surf. Coat. Technol.* 133–134 (2000) 61.
- [11] J. Stockemer, R. Winand, P. Vanden Brande, *Surf. Coat. Technol.* 115 (1999) 230.
- [12] J.N. Tu, J.G. Duh, S.Y. Tsai, *Surf. Coat. Technol.* 133–134 (2000) 181.
- [13] G. Aldrich-Smith, D.G. Teer, P.A. Dearnley, *Surf. Coat. Technol.* 116–119 (1999) 1161.
- [14] L. Cunha, M. Andritschky, L. Rebouta, R. Silva, *Thin Solid Films* 317 (1998) 351.
- [15] I. Milosev, J.M. Abels, H.H. Strehblow, B. Navinsek, M. Metikos-Hukovic, *J. Vac. Sci. Technol., A* 14 (1996) 2527.
- [16] P. Pajan, B. Navinsek, A. Cvelbar, A. Zalar, I. Milosev, *Thin Solid Films* 281–282 (1996) 298.
- [17] I. Milosev, H.H. Strehblow, B. Navinsek, *Surf. Coat. Technol.* 74–75 (1995) 897.
- [18] P. Pajan, B. Navinsek, *Surf. Coat. Technol.* 74–75 (1995) 919.
- [19] K.H. Nam, M.J. Jung, J.G. Han, *Surf. Coat. Technol.* 131 (2000) 222.
- [20] C. Rebolz, H. Ziegele, A. Leyland, A. Matthews, *Surf. Coat. Technol.* 115 (1999) 222.
- [21] C. Meunier, S. Vives, G. Bertrand, *Surf. Coat. Technol.* 107 (1998) 149.
- [22] G. Berg, C. Friedrich, E. Broszeit, C. Berger, *Surf. Coat. Technol.* 86–87 (1996) 184.
- [23] O. Piot, C. Gautier, J. Machet, *Surf. Coat. Technol.* 94–95 (1997) 409.
- [24] I. Dorfel, W. Osterle, I. Urban, E. Bouzy, *Surf. Coat. Technol.* 111 (1999) 199.
- [25] R. Sanjines, P. Hones, F. Levy, *Thin Solid Films* 332 (1998) 225.
- [26] M. Van Stappen, L.M. Stals, M. Kerkhofs, C. Quaeys, *Surf. Coat. Technol.* 74–75 (1995) 629.
- [27] J. Creus, H. Idrissi, H. Mazille, F. Sanchette, P. Jacquot, *Surf. Coat. Technol.* 107 (1998) 183.
- [28] M. Bin-Sudin, A. Leyland, A.S. James, A. Matthews, J. Housden, B. Garside, *Surf. Coat. Technol.* 81 (1996) 215.

- [29] R. Rebolé, A. Martínez, R. Rodríguez, G.G. Fuentes, E. Spain, N. Watson, J.C. Avelar-Batista, J. Housden, F. Montalá, L.J. Carreras, T.J. Tate, *Thin Solid Films* 469–470 (2004) 466.
- [30] B.A. Movchan, A.V. Demchishin, *Fizika Metall.* 28 (1969) 653.
- [31] P.J. Burnett, D.S. Rickerby, *Thin Solid Films* 154 (1987) 403.
- [32] P.A. Steinmann, Y. Tardy, H.E. Hintermann, *Thin Solid Films* 154 (1987) 333.
- [33] J.C.A. Batista, C. Godoy, V.T.L. Buono, A. Matthews, *Mater. Sci. Eng., A Struct. Mater.: Prop. Microstruct. Process.* 336 (2002) 39.
- [34] K. Holmberg, A. Matthews, *Coatings Tribology*, Elsevier, Amsterdam, 1994.
- [35] S. Carrera, O. Salas, J.J. Moore, A. Woolverton, E. Sutter, *Surf. Coat. Technol.* 167 (2003) 25.